

## Research on Payne effect of natural rubber reinforced by graft-modified silica

Wen Fu, Li Wang

College of Chemical Engineering, Guangdong University of Petrochemical Technology, Maoming, Guangdong 525000, China  
Correspondence to: L. Wang (E-mail: wanglihaha@126.com)

**ABSTRACT:** Silica ( $\text{SiO}_2$ ) modified by *in situ* solid-phase grafting was used for natural rubber (NR) reinforcement. The physical mechanical properties and Payne effect of natural rubber reinforced by  $\text{SiO}_2$  and graft-modified silica (G- $\text{SiO}_2$ ) were analyzed systematically. The results showed the comprehensive performance of NR/G- $\text{SiO}_2$  was better than that of NR/ $\text{SiO}_2$ . There was a proportional relationship between the filler loading and Payne effect. NR/G- $\text{SiO}_2$  presented weaker Payne effect in comparison with NR/ $\text{SiO}_2$ . A qualitative analysis on the correlation of filler 3D network structure and filler loading was carried out according to the relationship between the bound rubber content and the shear modulus. The Payne effect mechanisms of rubber compounds differed according to the different filler loading. © 2016 Wiley Periodicals, Inc. *J. Appl. Polym. Sci.* **2016**, *133*, 43891.

**KEYWORDS:** grafting; mechanical properties; rubber; theory and modeling

Received 18 December 2015; accepted 28 April 2016

DOI: 10.1002/app.43891

### INTRODUCTION

Wet skid resistance, rolling resistance, and wear resistance were always considered as devil's triangle in tire industry, meaning that it was difficult to improve the performance of the three mentioned aspects by one method at the same time. In order to overcome these difficulties, silica had been prepared as the filler to produce energy-saving tires of limousine<sup>1</sup> which was integrated with environmental protection, energy saving, safety, and comfort. Moreover, this method not only solved black pollution caused by the carbon black filler, but also reduced the rolling resistance of 22–35%, and the skid resistance was excellent as well. Due to the excellent performance, more than half of silica had been applied to rubber industry. Particularly, precipitated silica had become the main reinforcing materials besides carbon black, which had been used as reinforcing filler partially or exclusively for NR,<sup>2</sup> epoxidized natural rubber (ENR),<sup>3</sup> styrene-butadiene rubber (SBR),<sup>4</sup> silicone rubber,<sup>5</sup> etc.

However, there were some problems to process silica reinforced rubber. First of all, due to the presence of lots of hydroxyl groups on its surface, silica was hydrophilicity, which results that it was hard to be wetted and dispersed in rubber matrix, especially for nonpolar rubber (such as natural rubber). Secondly, the nano-silica showed small size and high surface energy, which was prone to aggregation, and thus leading to a significant decrease of the processing performance and reinforcing properties when it was used to rubber reinforcement. So far, researchers had proposed some surface modification methods,

including surfactant modification,<sup>6</sup> silane coupling agent modification,<sup>7</sup> graft polymer modification<sup>8</sup> and so on, to improve the dispersion of silica and the compatibility in the polymer matrix. These methods played a good role in improving the reinforcing properties of silica.

However, the current research works focused on the choice of appropriate modifier and modification processes.<sup>6–8</sup> There were few studies on the mechanism of silica-reinforced rubber, such as Payne effect mechanism. For the Payne effect, Payne himself explained that the Payne effect was due to the destruction of the physical interaction between the fillers.<sup>9</sup> Many studies had evolved the view of Payne and presented various filler network models, such as Kraus model,<sup>10</sup> VTG model,<sup>11</sup> NJ model<sup>12</sup> and so on. Moreover, Cassagnau<sup>13</sup> and Sternstein<sup>14</sup> indicated that the disentanglement of polymer molecular chain was connected with Payne effect. In fact, the mechanism of the impact of filler on the dynamic viscoelastic properties of rubber was very complex, and it was not entirely clear until now. As for rubber material filled by silica, energy dissipation would occurred because of the break and reconstruction of filler network during the cyclical strain, thus influencing the performance of rubber materials, such as dynamic heat buildup. As a result, studies on the characteristics of the filler network in rubber matrix were very important to enhance the performance of rubber material.

In this paper, the graft-modified silica was used to reinforce natural rubber, and its physical mechanical properties were studied, focusing on the influence of the filler type and loading

**Table I.** Impact of Modified Silica on Physical Mechanical Properties of Natural Rubber

Performance	Before modification	After modification	Elevation ratio (%)
Tensile strength (MPa)	15.2	21.7	42.7
Stretching stress (300%) (MPa)	4.1	6.7	63.4
Tear strength (kN/m)	30.3	53.5	76.6
Elongation at break (%)	700	594	-15.1
Resilience (25 °C)	35	36	2.9
Roller abrasion (absolute abrasion) (g)	0.76	0.40	90.0
Grade 6 flex cracking resistance (10 <sup>4</sup> times)	11.40	15.01	31.7

on the Payne effect of natural rubber. Importantly, the Payne effect mechanism of rubber was discussed.

## EXPERIMENTAL

### Materials and Equipments

Precipitated silica (~50 nm), bis-( $\gamma$ -triethoxysilylpropyl)-tetrasulfide (Si-69), natural rubber (trademark: 3L, Vietnam), N-isopropyl-N'-phenyl-p-phenylenediamine (4010NA) antioxidant, ZnO, stearic acid, 2,2'-dibenzothiazole disulfide (DM) accelerant, and sulfur were bought directly from the market and used without purification. Scanning electron microscope (SEM), LEO1530VP, LEO Company in Germany. Torque rheometer, HAKKE400P, Thermo Electron in USA. Rubber Process Analyzer (RPA), RPA2000, the Alpha Technologies Company in USA.

### Sample Preparation

NR was added to a two-roll mill with the roller spacing of 1 mm. Eight minutes later, the silica, Si-69, antioxidant 4010NA, ZnO, stearic acid were added successively, followed by five times side cuts at both the left and right, and a triangle package was implemented 3 times. Then the mix was treated in a HAAKE rheomix for 8 min with a rotor speed of 60 rpm and a temperature of 120 °C in order to make G-SiO<sub>2</sub>.<sup>15,16</sup> Then DM and sulfur were added to the mix with a two-roll mill at room temperature. After the feeding was completed, followed by five times side cuts at both the left and right. Finally, a triangle package was implemented 8 times and thin-passing for 8 times. Exported slices were allowed to stand for above 16 h and

then vulcanized on a press vulcanizer at 150 °C with 16 MPa for  $t_{90} + 2$  min.

The formulation was as follows: NR 100 phr, ZnO 5 phr, stearic acid 2 phr, antioxidant 4010NA 1 phr, DM 1 phr, sulfur 2 phr, the filler content for variable 10–50 phr, the dosage of Si-69 was 8% of the filler content.

### Characterization and Test

The shear modulus was tested by Alpha Technologies RPA2000 rubber processing analyzer, and the test conditions were shown as the following. The tensile properties were tested according to GB/T 528-2009, dumbbell-shaped specimens, the thickness of 2.0 mm. The tear strength was tested according to GB/T 529-2008, right angle specimens, the thickness of 2.0 mm. The resilience was tested according to GB/T 1681-2009. The abrasion was tested according to GB/T 9867-2008. The flex cracking resistance was tested according to GB/T 13934-1992. SEM was using with a magnification times of 20–90000 $\times$ , an acceleration voltage of 0.1–30 kV, and the specimens surfaces were sprayed with gold. The bound rubber test conditions: after 1 day at room temperature, rubber compounds sample of  $0.5000 \pm 0.0002$  g( $m_1$ ) was segmented into small pieces of about 1 mm<sup>3</sup>, then wrapped by 600 mesh steel mesh. The prepared samples were immersed into toluene solvent at room temperature for 3 days, and the solvent was renewed once a day. Finally, the samples were dried to constant weight ( $m_2$ ), bound rubber was calculated according to the following formula:

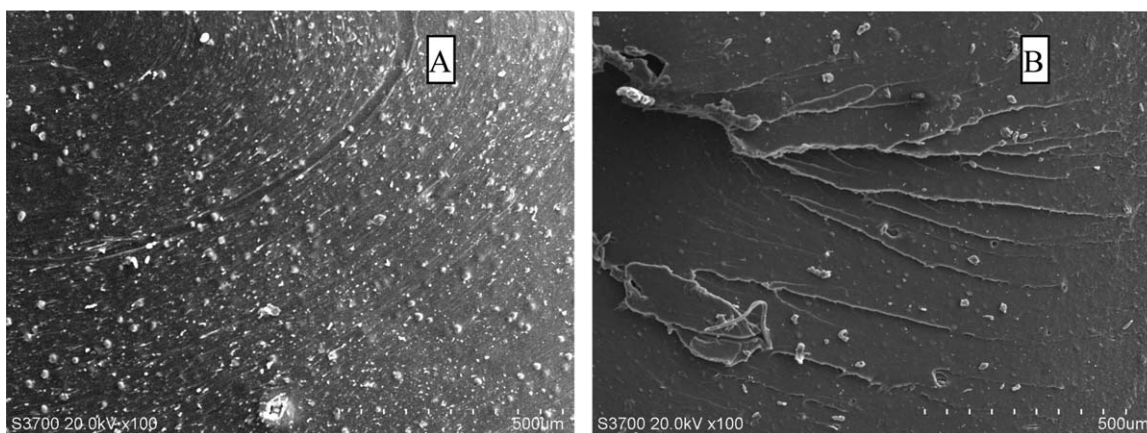


**Figure 1.** The morphology of tensile fracture surface of NR/SiO<sub>2</sub> and NR/G-SiO<sub>2</sub>.

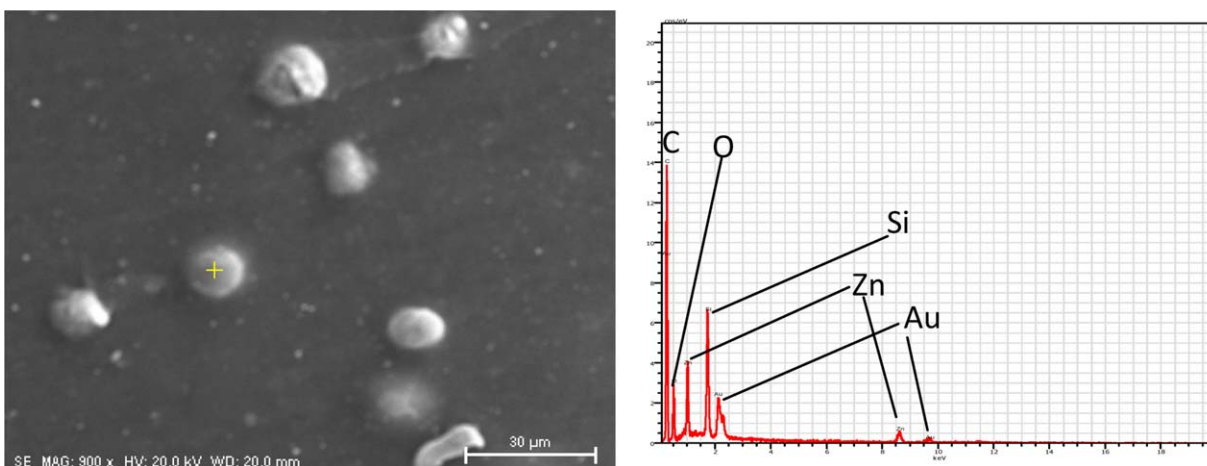


**Figure 2.** The electron spectroscopy analysis of the tensile fracture surface of NR/SiO<sub>2</sub>. [Color figure can be viewed in the online issue, which is available at [wileyonlinelibrary.com](http://wileyonlinelibrary.com).]

$$m = \frac{m_2 - m_1 \omega_2}{m_1 \omega_1} \times 100\% \quad (1)$$

where  $m$  is the amount of bound rubber;  $\omega_1$  is rubber loading in the rubber compounds sample (wt. %);  $\omega_2$  is filler loading in the rubber compounds sample (wt. %).

## RESULTS AND DISCUSSION

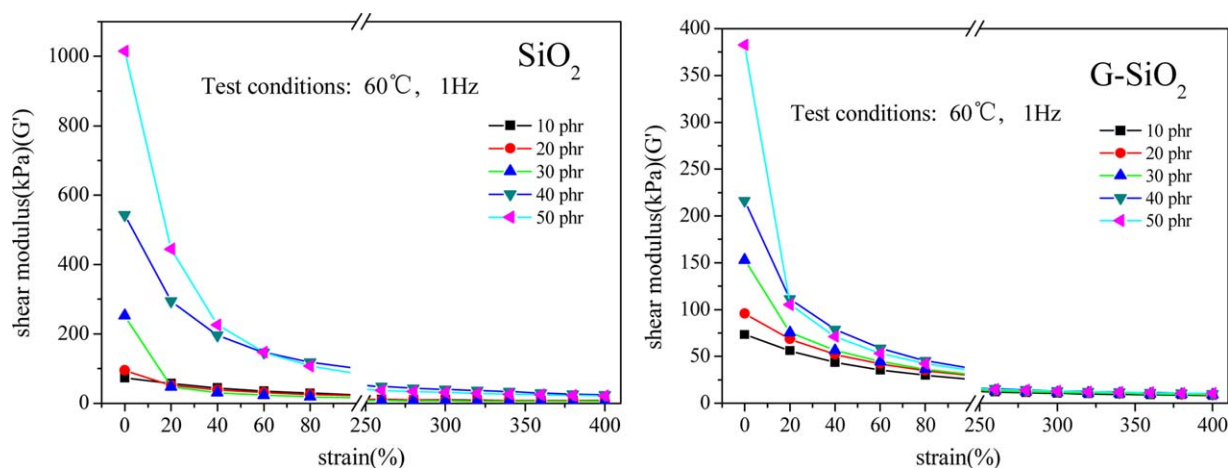
### Influence of Modified Silica on Physical Mechanical Properties of Natural Rubber

Table I exhibited the influence of G-SiO<sub>2</sub> on reinforcing properties of natural rubber (filler content 50 phr). Compared with NR/SiO<sub>2</sub> vulcanizate, the tensile strength, 300% stretching stress and tear strength of NR/G-SiO<sub>2</sub> vulcanizate all increased over 40%, while a 32% increase of grade 6 flex cracking resistance and a slightly ascending of resilience were also observed. After modification, absolute quality abrasion decreased from 0.76 to 0.40 g, wear resistance increased nearly one times. Although a slightly decrease was observed in elongation at break, it always maintained a high level of 594%. This enhancing property could be attributed to the reaction between Si-69 and hydroxyl groups at surface of silica, which conducted to the improvement of the

dispersion of silica in rubber matrix and the compatibility of silica and rubber matrix, and thus improved the performance of the rubber compounds.

### Microstructure of NR/SiO<sub>2</sub> and NR/G-SiO<sub>2</sub>

Figure 1 shows the morphology of tensile fracture surface of NR/SiO<sub>2</sub> [Figure 1(A)] and NR/G-SiO<sub>2</sub> [Figure 1(B)] (filler content 50 phr). The fracture surface of NR/SiO<sub>2</sub> vulcanizate was relatively clear and smooth, which implied that the interface interaction between the filler and the matrix was weak, resulting in the occurrence of fracture at the interface between the two phase under the external force. By contrast, the fracture surface of NR/G-SiO<sub>2</sub> vulcanizate was rougher. This phenomenon demonstrated that the interface interaction between the filler and the matrix was enhanced after the addition of modified silica. Meanwhile, many obvious high spots were found on the fracture surface of NR/SiO<sub>2</sub> vulcanizate, while just a little was observed on the fracture surface of NR/G-SiO<sub>2</sub> vulcanizate. The following EDS analysis [Figure 2] indicated the high spots in the figure were the aggregate of silica. In other words, the



**Figure 3.** Variation of shear modulus vs. strain with different silica loading. [Color figure can be viewed in the online issue, which is available at [wileyonlinelibrary.com](http://wileyonlinelibrary.com).]

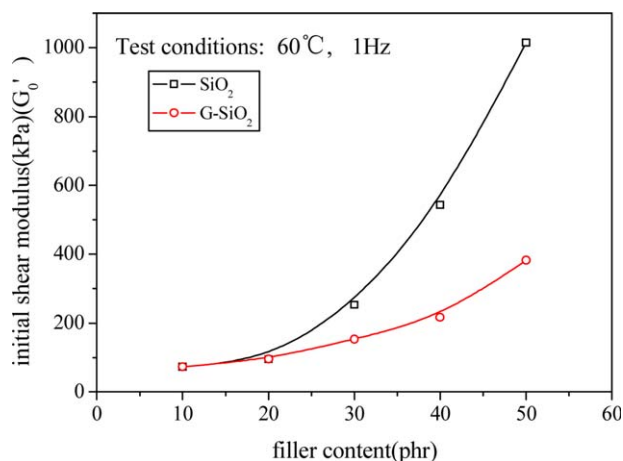


**Figure 4.** Variation of initial shear modulus  $G'_0$  with different silica loading. [Color figure can be viewed in the online issue, which is available at [wileyonlinelibrary.com](http://wileyonlinelibrary.com).]

addition of modifier played a significant role in improving the silica dispersion in the rubber matrix.

#### Influence of Content of Silica on the Rubber Compounds' Payne Effect

Figure 3 shows the shear modulus ( $G'$ ) of rubber compounds with different silica loading from 10 to 50 phr. All samples with different silica loading presented a similar trend: As the strain increased, a gradual decline was observed in the shear modulus of rubber compounds, followed by a stable value. In other words, with different filler loading, rubber compounds exhibited a certain degree of Payne effect. Particularly, the increasing filler loading resulted in a more distinct Payne effect. This phenomenon could be attributed to two factors: at a low silica loading, the particles with large distance would lower the possibility of gathering to form the filler 3D network structure; on the other hand, excess silica loading would form the filler 3D network structure, leading to an increase in the shear modulus of rubber

compounds. While a high strain would destroy the formative filler 3D network, following by the rapid decline of the shear modulus. With further increasing strain, the filler 3D network structure would be destroyed completely, and no obvious change of the shear modulus was found, leading to platform under the strain of 350–400%.<sup>17</sup>

In addition, the initial shear modulus of the rubber compounds ( $G'_0$ ) was consisted of matrix viscoelasticity ( $G'_p$ ), filler-polymer interactions ( $G'_h$ ), and filler-filler interactions ( $G'_n$ ).<sup>18</sup>  $G'_p$  is related to the cross-linked structure and the nature of the rubber, while  $G'_h$  is related to filler-polymer interactions.  $G'_n$  is related to the network structure of the filler. Difference in  $G'_p$  would be not obvious once the rubber type and the content of cross-linking agent being equal. Thereby, the influence of  $G'_p$  on  $G'_0$  could be ignored in the following work.  $G'_0$  was mainly defined by  $G'_h$  and  $G'_n$ ,  $G'_0 = G'_h + G'_n$ . The filler 3D network structure of rubber compounds would not be damaged under the strain of 0%. Here, the relationship of filler-polymer interactions and filler-filler interactions was expressed by  $G'_0$  ( $\lambda = 0\%$ ). The  $G'_0$  of rubber compounds with the same loading of SiO<sub>2</sub> and G-SiO<sub>2</sub> were compared in Figure 4. Both  $G'_0$  of rubber compounds gradually increased with the increase of filler loading. Particularly, there were no obvious difference between  $G'_0$  (SiO<sub>2</sub>) and  $G'_0$  (G-SiO<sub>2</sub>) when the filler loading varied at 10–20 phr. Because it was less likely to form filler 3D network structure at low content of filler, so both  $G'_n$  (G-SiO<sub>2</sub>) and  $G'_n$  (SiO<sub>2</sub>)  $\approx 0$ , thus  $G'_0$  mainly relied on  $G'_h$ . The interaction between rubber matrix and G-SiO<sub>2</sub> was higher than that between rubber matrix and SiO<sub>2</sub>, so  $G'_h$  (G-SiO<sub>2</sub>)  $>$   $G'_h$  (SiO<sub>2</sub>), and hence  $G'_0$  (G-SiO<sub>2</sub>)  $>$   $G'_0$  (SiO<sub>2</sub>). While for filler loading of  $>20$  phr, the space of filler particle decreased, and filler 3D network structure began to form. When  $G'_n$  performed a dominant role in  $G'_0$  of rubber compounds. After the addition of modified silica, the dispersion in the rubber matrix would raise, and the filler 3D network structure of rubber compounds should be weakened, which led to  $G'_n$  (G-SiO<sub>2</sub>)  $<$   $G'_n$  (SiO<sub>2</sub>), and therefore  $G'_0$  (G-SiO<sub>2</sub>)  $<$   $G'_0$  (SiO<sub>2</sub>).

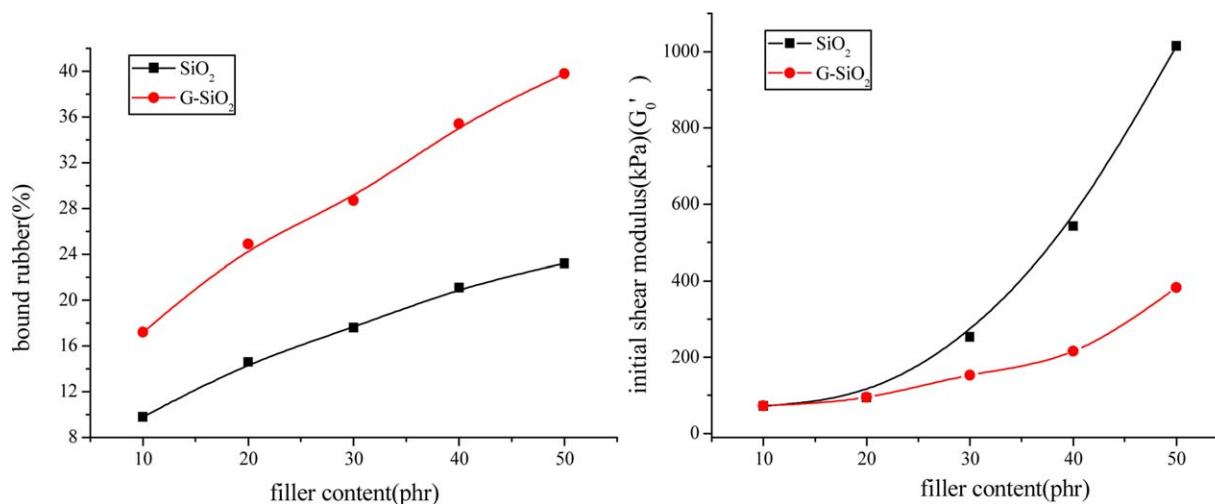


**Figure 5.** Relationship between bound rubber content and initial shear modulus  $G'_0$  with different silica loading. [Color figure can be viewed in the online issue, which is available at [wileyonlinelibrary.com](http://wileyonlinelibrary.com).]



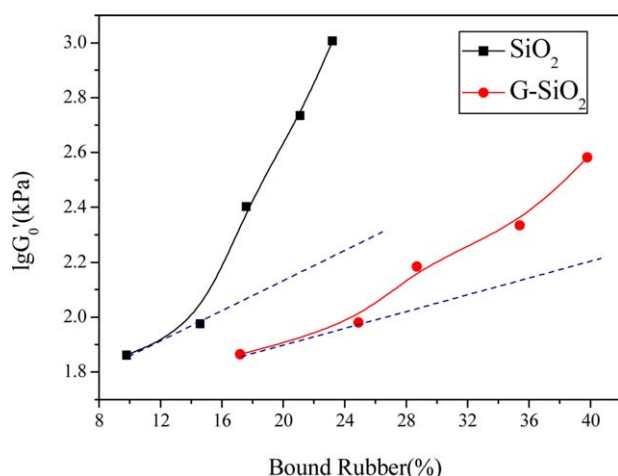


**Figure 6.** Bound rubber- $\lg G_0'$  relation curves. [Color figure can be viewed in the online issue, which is available at [wileyonlinelibrary.com](http://wileyonlinelibrary.com).]

### Relationship between Bound Rubber and Shear Modulus of Rubber Compounds

As above mentioned  $G_0' = G'h + G'n$ , in which  $G'h$  could be expressed by the bound rubber of rubber compounds. Thus, the relationship between bound rubber and initial shear modulus of rubber compounds could explore the network structure of  $\text{SiO}_2$  and  $\text{G-SiO}_2$  with different loading.

Figure 5 shows the bound rubber and the initial shear modulus of samples with different filler loading. Both the bound rubber and the initial shear modulus of rubber compounds raised with the increase of filler loading. However, there were some differences between their rising trends. Especially, for the filler loading higher than 40 phr,  $G_0'$  of rubber compounds with  $\text{SiO}_2$  always performed significantly higher than that with  $\text{G-SiO}_2$ , which could be attributed to the formation of filler 3D network structure.

In order to represent the influence of the filler 3D network structure on  $G_0'$  of rubber compounds intuitively, the curve of bound rubber- $\lg G_0'$  was shown in Figure 6. If there was no or

little effect of filler 3D network structure on  $G_0'$ , the curve should approximate a straight line (as shown by the dotted line, the extension of the connection line of samples with the content of 10 and 20 phr. Generally, it was less likely to form the filler network structure at such a low filler loading). The increasing deviation between the solid line and dotted line indicated the formation of more filler 3D network structure. When filler loading varied from 30 to 50 phr, a certain degree of deviation was observed, indicating the formation of filler 3D network structure. With further increasing filler, the deviation degree grew, and more filler 3D network structure was formed. Moreover, a smaller deviation between the solid line and its corresponding dotted line could be observed in rubber compounds with  $\text{G-SiO}_2$ , which indicated that  $\text{G-SiO}_2$  in the rubber matrix dispersed better than  $\text{SiO}_2$ , thereby less filler 3D network structure.

### Relationship between Network Chain Ultimate Elongation of Vulcanizate and Payne Effect

Figure 7 shows the reciprocal of strain ( $\lambda^{-1}$ ) vs. the reduced stress ( $\frac{\sigma}{\lambda - \lambda^{-2}}$ ) curves of  $\text{SiO}_2$ - and  $\text{G-SiO}_2$ -filled NR under different filler contents. The reduced stress of all samples reduced first and then increased with the increase of strain, which actually reflected two additional effects in the stretching process: at low strain, the reduced stress decreased with the increasing of strain, which could be attributed to the Payne effect of materials; while at high strain, the reduced stress performed the opposite trend, due to the network chain ultimate elongation resulting from non-Gaussian effects.<sup>19</sup>

Also, the reduced stress of NR/ $\text{SiO}_2$  vulcanizate and NR/ $\text{G-SiO}_2$  vulcanizate showed diverse trend with the change of strain. In order to intuitively compare the difference of Mooney plots of vulcanizate with and without modified silica, three samples with filler loading of 10, 30, and 50 phr were shown in Figure 8. At 10 phr [Figure 8(a)], no obvious decrease could be found in the region of the low strain. That fact could be attributed to the favorable dispersibility of the two samples in the rubber matrix, leading to the unobvious Payne effect. As the filler loading increased to 30 phr [Figure 8(b)] or 50 phr [Figure 8(c)], the Mooney plots of vulcanizate with  $\text{SiO}_2$

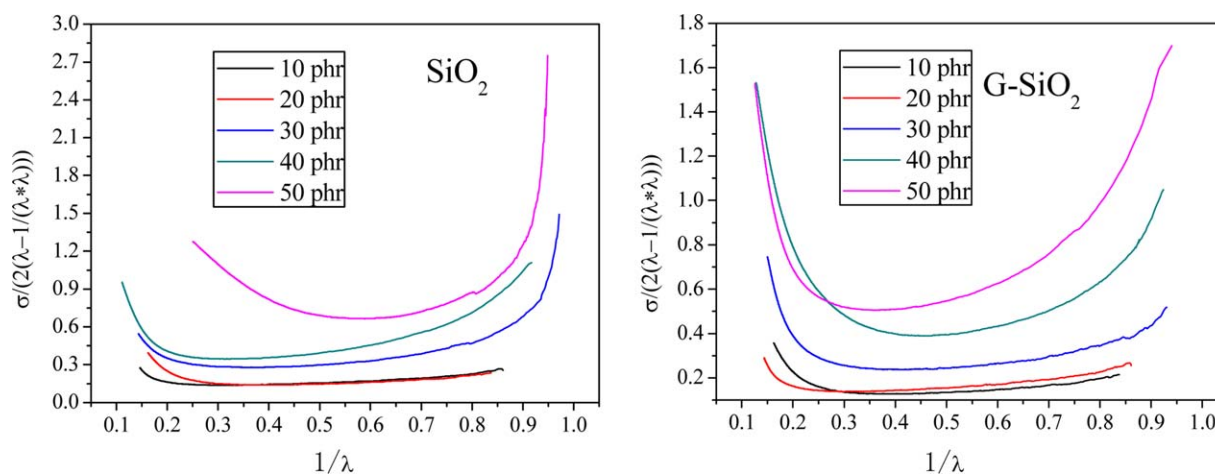


**Figure 7.** Mooney curves of natural rubber for various silica contents. [Color figure can be viewed in the online issue, which is available at [wileyonlinelibrary.com](http://wileyonlinelibrary.com).]

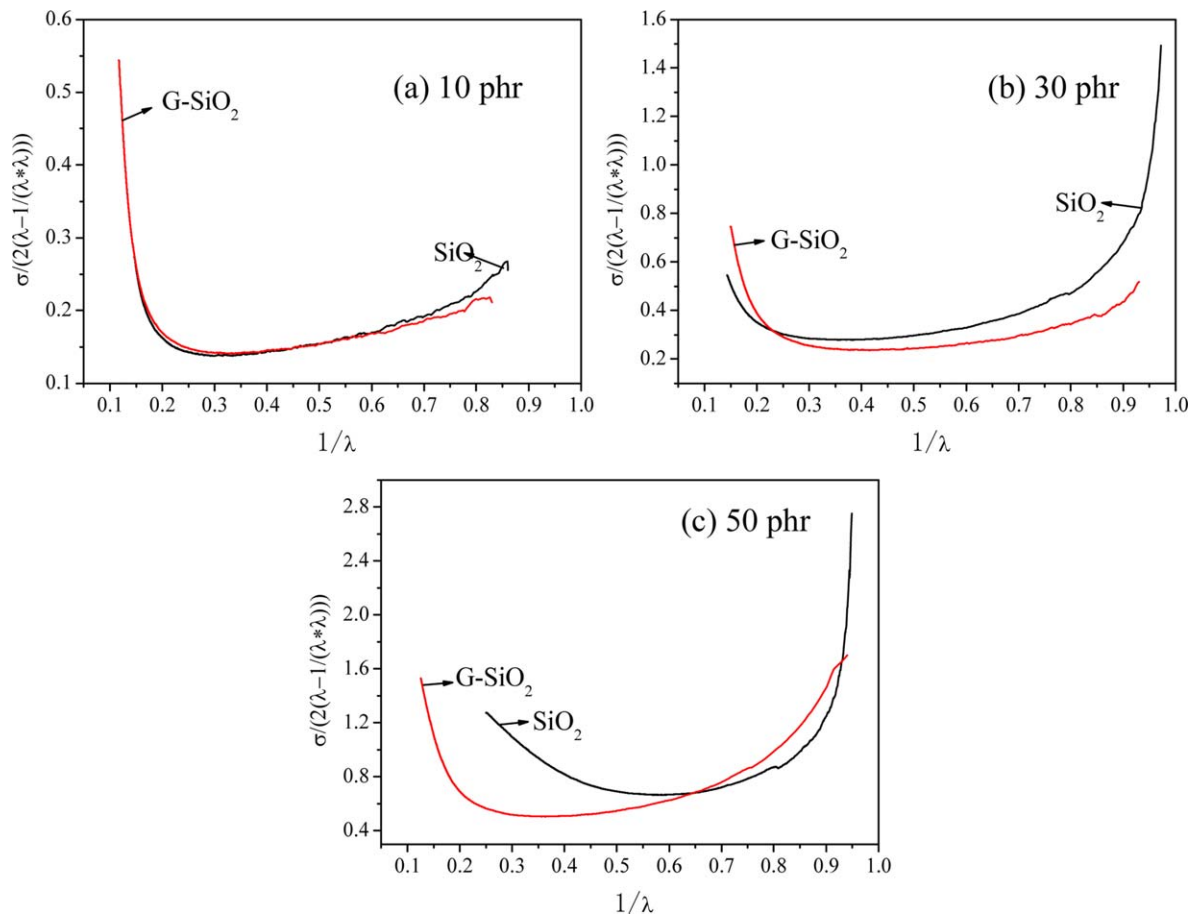


Figure 8. Mooney plots of  $\text{SiO}_2$  and G- $\text{SiO}_2$ -filled NR. [Color figure can be viewed in the online issue, which is available at wileyonlinelibrary.com.]

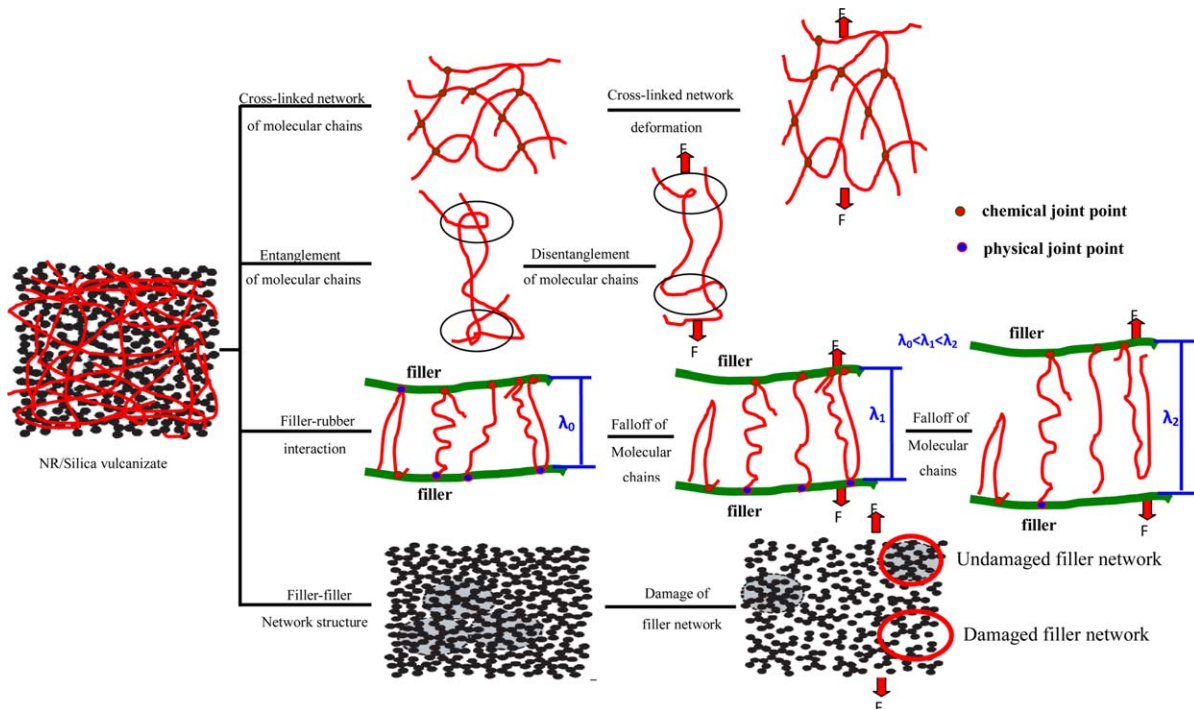


Figure 9. Payne effect mechanisms of silica-filled NR. [Color figure can be viewed in the online issue, which is available at wileyonlinelibrary.com.]

decreased more significantly than vulcanizate with G-SiO<sub>2</sub> in the region of the low strain, implying that Payne effect of vulcanizate with SiO<sub>2</sub> was more intense than the nonmodified counterparts. The modified silica dispersed more uniform than the nonmodified counterparts in the rubber matrix, and less filler 3D network structure was formed at the same filler loading. Both the Mooney plots of the two vulcanizates increased with the increase of strain in the region of the high strain. However, the rising trend of the Mooney plots of the vulcanizate with modified silica was more evident than that with their nonmodified counterparts, indicating that ultimate elongation effect of the vulcanizate with modified silica was more intense. The modified silica dispersed more uniform than silica in the rubber matrix, and thus more filler-polymer interaction points were formed, resulting in more intense ultimate elongation effect.

#### Mechanisms of Payne Effect of Natural Rubber/Silica

Based on Roozbeh and Mikhail's<sup>20</sup> findings on filler reinforced rubber, several different structures might exist in the filler reinforced rubber system, including the chemical cross-linked network structure of the rubber molecular chains caused by cross-linking agents, the physical entanglement molecular chains of the rubber molecular chains, the filler-rubber interactions structure from rubber molecular chain, silica surface through physical adsorption or chemical combination and filler 3D network structure by filler aggregation. The Payne effect of material was precisely attributed to the comprehensive function of these multiple factors under stress-strain.

Based on above work, the Payne effect mechanisms of natural rubber/silica under different conditions were predicted as follows: (a) at nonfilled reinforced rubber system, the Payne effect was mainly due to the disentanglement of rubber molecular chain; (b) at filler reinforced rubber system with low filler content, the Payne effect was contributed mainly by rubber molecular chain slippage or detachment from silica surface. Molecular chain of rubber adsorbed at the two fillers had different length. At low strain (as shown in Figure 9 when the strain is  $\lambda_1$ ), the Payne effect mainly expressed molecular chains slippage, if the molecular chains between filler did not reach ultimate elongation. The mainly performance of Payne effect was molecular chains of rubber detached from silica surface, if the molecular chains between the fillers reached ultimate elongation. While, with further increasing strain (as shown in Figure 9 when the strain is  $\lambda_2$ ), molecular chains detached from the silica surface when more rubber molecular chains in fillers reached ultimate elongation, following by further rising of Payne effect; (c) at filler reinforced rubber system with high filler content, filler network structure began to form, when the Payne effect was mainly attributed to the destruction of the filler aggregates during strain process. The Payne effect caused by the destruction of filler aggregates was stronger than that of molecular chain slippage and detachment.

#### CONCLUSIONS

Natural rubber with different silica loading performed Payne effect, and the Payne effect became more strongly with the increasing silica loading. The Payne effect of modified silica

reinforced natural rubber was weaker than their nonmodified counterparts. The modified silica had better compatibility with the rubber matrix than nonmodified silica, a well dispersibility in the rubber matrix, thus generating less filler 3D network structure. At nonfilled reinforced rubber system, the Payne effect was mainly due to the disentanglement of rubber molecular chain; at filler reinforced rubber system with low filler content, the Payne effect was mainly due to molecular chain slippage and detachment from silica surface; at filler reinforced rubber system with high filler content, the Payne effect could be attributed to the destruction of filler 3D network structure.

#### ACKNOWLEDGMENTS

This research was supported by Guangdong University of Petrochemical Technology, Scientific Research Fund (No. 650115) and Natural Science Foundation of Guangdong Province, China (No. 2015A030313766).

#### REFERENCES

- Bertora, A.; Castellano, M.; Marsano, E.; Alessi, M.; Conzatti, L.; Stagnaro, P.; Colucci, G.; Priola, A.; Turturro, A. *Macromol. Mater. Eng.* **2011**, 296, 2011.
- Tunlert, A.; Prasassarakich, P.; Poompradub, S. *Macromol. Symp.* **2015**, 354, 62.
- Xu, T. W.; Jia, Z. X.; Luo, Y. F.; Jia, D. M.; Peng, Z. *Appl. Surf. Sci.* **2015**, 328, 306.
- Wang, S. T.; Cen, L.; Wu, Q. H. *Polym. Adv. Technol.* **2015**, 26, 953.
- Mariot, D.; Caro-Bretelle, A.; Lenny, P.; Ganachaud, F. *Polym. Int.* **2015**, 64, 1128.
- Ismail, H.; Ishiaku, U. S.; Ishak, Z. A. M.; Freakley, P. K. *Eur. Polym. J.* **1997**, 33, 1.
- Yamazaki, R.; Karyu, N.; Noda, M.; Fujii, S.; Nakamura, Y. *J. Appl. Polym. Sci.* **2016**, 133, DOI: 10.1002/app.43256.
- Rezaei, S.; Pourabbas, B. *Polym. Compos.* **2015**, 36, 1365.
- Payne, A. R. *J. Appl. Polym. Sci.* **1962**, 57, 6.
- Kraus, G. *J. Appl. Polym. Sci.* **1984**, 39, 75.
- Van de Walle, A.; Tricot, C.; Gerspacher, M. *Kautsch. Gummi Kunstst* **1996**, 49, 172.
- Heinrich, G.; Klüppel, M. *Adv. Polym. Sci.* **2002**, 160, 1.
- Cassagnau, P. *Polymer* **2003**, 44, 2455.
- Sternstein, S. S.; Zhu, A. *J. Macromol.* **2002**, 35, 7262.
- Karnda, S.; Kannika, S.; Wilma, K. D.; Jacques, W. M. *Eur. Polym. J.* **2014**, 51, 69.
- Ansarifar, A.; Wang, L.; Ellis, R. J.; Kirtley, S. P.; Riyazuddin, N. *J. Appl. Polym. Sci.* **2007**, 105, 322.
- Rwei, S. P.; Manas-Zloczower, I.; Feke, D. L. *Polym. Eng. Sci.* **1991**, 31, 558.
- Frohlich, J.; Niedermeier, W.; Luginsland, H. D. *Compos. Part A: Appl. Sci.* **2005**, 36, 449.
- Meissner, B.; Matejka, L. *Polymer* **2000**, 41, 7749.
- Roozbeh, D.; Mikhail, I. *Int. J. Solids Struct.* **2009**, 16, 2967.